ANTICANCER RESEARCH *24*: 907-920 (2004)

Antitumor Activity of Imidazothioxanthones in Murine and Human Tumor Models *In Vitro* and *In Vivo*

A. VARVARESOU[2], K. IAKOVOU[2], E. GIKAS[2], I. FICHTNER[3#], H.H. FIEBIG[4#], L.R. KELLAND[5#], J.A. DOUBLE[6#], M.C. BIBBY[6#] and H.R. HENDRIKS[1]

[1]*EORTC New Drug Development Office, Amsterdam, The Netherlands;*
[2]*University of Athens, School of Pharmacy, Department of Pharmaceutical Chemistry, Athens, Greece;*
[3]*Experimental Pharmacology, Max-Delbrück Center for Molecular Medicine, Berlin;*
[4]*Institute for Experimental Oncology, Oncotest GmbH, Freiburg, Germany;*
[5]*CRC Centre for Cancer Therapeutics, The Institute of Cancer Research, Sutton;*
[6]*Cancer Research Unit, University of Bradford, U.K.; # for the Screening and Pharmacology Group of the EORTC*

Abstract. *Background: A new series of imidazothioxanthones has recently been synthesized as potential anticancer agents with the aim of overcoming drug resistance. The route of synthesis and DNA-binding properties of the compounds were reported previously. This paper describes the general structure-activity relationships for the class of imidazothioxanthones in panels of human and murine tumor cell lines in vitro, and the in vivo activity against human and murine solid tumors of the most potent compound, N-[3-(Dimethylamino)propylo]-11-oxo-11H-benzothiopyrano [3',2': 2, 3]pyrido[1,2-a] imidazo-2-carboxamide (10a). In addition, the interaction between compound 10a and DNA is also considered in terms of molecular mechanics methods and flexible docking techniques. Materials and Methods: The cytotoxicity of compounds 10a, 11-oxo-N-[2-(pyrrolidino)ethylo]-11H-benzothiopyrano [3',2':2,3]pyrido[1,2-a] imidazo-2-carboxamide, 11-oxo-N-[2-(piperidino)ethylo]-11H-benzothiopyrano [3',2':2,3]pyrido[1,2-a] imidazo-2-carboxamide and N-[2-(morpholino)ethylo]-11-oxo-11H-benzothiopyrano [3',2': 2, 3]pyrido[1,2-a]imidazo-2-carboxamide (10c-10e) was assessed in human tumor cell lines and xenografts using the sulforhodamine B assay, MTT assay and the clonogenic assay. The human ovarian xenograft, PXN/109TC, two human breast carcinomas, MT-1 and MCF-7, and the murine colon adenocarcinoma, MAC 15A were used for the in vivo testing of compound 10a. In addition, the interaction between compound 10a and DNA is also considered in terms of molecular mechanics methods and flexible docking techniques. Results: Two compounds, 10a and 10c, showed cytotoxic activity below 10 mM in the NCI in vitro screen of 60 human tumor cell lines. The IC_{50} value of compound 10a was 6.8 mM and that of 10c, 8.3 mM. In addition, both compounds possessed differential activity against leukemia, colon and mammary cancer. The activity pattern was confirmed in two further screens using monolayer and clonogenic assays. In vivo antitumor studies showed that 10a was active against the human mammary carcinoma MT-1 and murine colon cancer MAC15A. Marginal activity was observed in human ovarian cancer model PXN/109T/C and the compound was inactive in human mammary cancer MCF-7. Conclusion: The results warrant further in vivo testing of 10a in additional human solid tumor models. The molecular modeling showed that the planarity of the chromophore and the side-chain conformation could assist the insertion of compound 10a between the base pairs of the double helix. On the other hand, docking to the nucleotide sequence GGAATTGCCTCA suggested that the molecule could also act as a minor groove binder.*

Correspondence to: Dr. A. Varvaresou, The School of Health & Caring Professions, Department of Aesthetics, Technological Education Institution, Ag. Spyridonos Str., GR-12210 Egaleo, Athens, Greece. Tel/Fax: +302106810354, e-mail: varvaresou@pharm.uoa.gr or Dr H. Hendriks, Hendriks Pharmaceutical Consulting, Wagenaarstraat 67, 1443 LR Purmerend, The Netherlands. e-mail: hr.hendriks@planet.nl

Key Words: Imidazothioxanthones, cytotoxicity, antitumor activity, human tumor xenografts, murine tumors, molecular modeling-docking.

Several classes of compounds including the anthracendiones (1), anthrapyrazoles (2,3), thioxanthones (4), (aza)acridine-4-carboxamides (5-7), (aza)dibenzodioxin-1-carboxamides (8,9), phenazine-1-carboxamides (10) and pyrido-, pyrazino-, imidazo-, pyrrolo-, pyrazolophenazinecarboxamides (11) can be distinguished among the currently recognized synthetic antineoplastic compounds designed as "DNA complexing agents". The main aim of the research for new structures within the mentioned groups was not only to develop synthetic compounds with antitumor activity, but to overcome the "intrinsic resistance" of many carcinoma cell lines to common agents compared to leukemia cell lines.

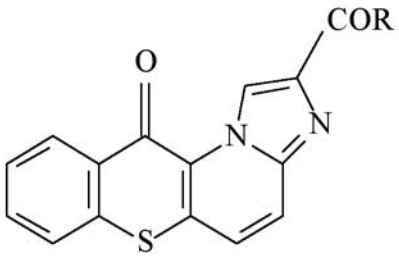

9, 10a-e

No	R
9	OC_2H_5
10a	$NH(CH_2)_3N(CH_3)_2$
10b	$NH(CH_2)_3N(C_2H_5)_2$
10c	$NH(CH_2)_2$ N
10d	$NH(CH_2)_2$ N
10e	$NH(CH_2)_2$ N O

Figure 1. *Chemical structures of compounds 9, 10a-e.*

As a part of research devoted to the investigation of new groups of antitumor DNA-interacting agents, recently we reported the synthesis, DNA-binding properties and preliminary *in vitro* data of the imidazothioxanthones 9 and 10a-e (12, Figure 1). These imidazothioxanthones, with the exception of the ester 9, possessed remarkable *in vitro* activity and DNA-binding properties, compounds 10a and 10c being the most interesting. This paper discusses the general structure-activity relationships *in vitro* for this series of imidazothioxanthones and the *in vivo* activity against human and murine solid tumors of the compound 10a.

In order to understand the binding mode of compound 10a, we examined, in terms of molecular modeling techniques, the geometry of the chromophore, the conformation of the side-chain and the interactions of the molecule with different sequences of base pairs.

Materials and Methods

Substances. All compounds were synthesized at the Department of Pharmaceutical Chemistry, School of Pharmacy, University of Athens (Greece).

In vitro cytotoxicity studies. The cytotoxicity of compounds 10a, 10c-10e was assessed in human tumor cell lines and xenografts using the sulforhodamine B assay (13,14), MTT assay (15,16) and the clonogenic assay (17,18).

The cytotoxicity profile of all compounds was evaluated in the *in vitro* screen of the National Cancer Institute (NCI) consisting of 60 human cancer cell lines. Detailed descriptions of the standard technical procedures and data analyses have been published elsewhere (13,14). Briefly, the assay involves plating the cells, pre-incubation for 24 h, followed by a 48-h continuous drug exposure over a broad concentration range (10^{-4}-10^{-9} M) using five 10-fold dilutions against a panel of 60 cell lines comprising nine tumor types. The cytotoxicity was assessed with the sulforhodamine B protein assay. Dose-response curves for each cell line and each compound were determined and also the following parameters: GI_{50}, TGI and LC_{50}. GI_{50} is the concentration inhibiting cell growth by 50% compared with control, TGI the concentration resulting in total growth inhibition, and LC_{50} the concentration causing 50% reduction in number of tumor cells at the end of the drug incubation, compared with that at the beginning. The results were also presented in mean graphs, creating a characteristic cell line fingerprint for each individual drug. Furthermore, the COMPARE algorithm was used to investigate whether the profiles of the compounds had a certain degree of similarity with other compounds with a known mechanism of action.

Furthermore, the *in vitro* activity of the compounds was tested in a representative murine and human cell line panel comprising leukemia (WEHI, K-562), colon (MAC15A, DLD-1) and the mammary cancer cell line MCF-7/ADR using a monolayer assay system (15,16). Briefly, 2000 cells/well were plated 24h prior to drug addition and the drug was added in eight serial dilutions of 10 starting at 100 μM. Drug stocks were formulated in DMSO. Cell growth was quantified by measuring the ability of viable cells to convert MTT into formazan after 6-day or 4-day continuous exposure to drug. Results are depicted as ±SE (n=6) percent of vehicle control. Optical density of vehicle control cells was set to be 100%. The results are presented as drug concentration necessary to achieve 50% growth inhibition, IC_{50}.

Further characterization of the *in vitro* cytotoxicity profiles of the compounds was carried out in human tumor xenografts using the clonogenic assay with continuous drug exposure. A modification of the double-layer soft-agar assay as described by Hamburger and Salmon (17) was used (18). Solid human tumor xenografts were mechanically disaggregated and subsequently incubated with an enzyme cocktail consisting of collagenase 0.05%, DNAse 0.07% and hyaluronidase 0.1 in RPMI 1640 at 37˚C for 30 min. The cells were washed twice and passaged through sieves of 200 and 50 mm each. The percentage viable cells was determined in a hemocytometer using trypan blue exclusion. The tumor cell suspension was plated into 24-well plates over a bottom layer consisting of 0.2 ml Iscoves' modified Dulbecco's medium with 20% fetal calf serum and 0.7% agar. Next 20,000 to 200,000 cells were added to 0.2 ml of the same culture medium and 0.4% agar and plated onto the base layer. Test compounds were applied by

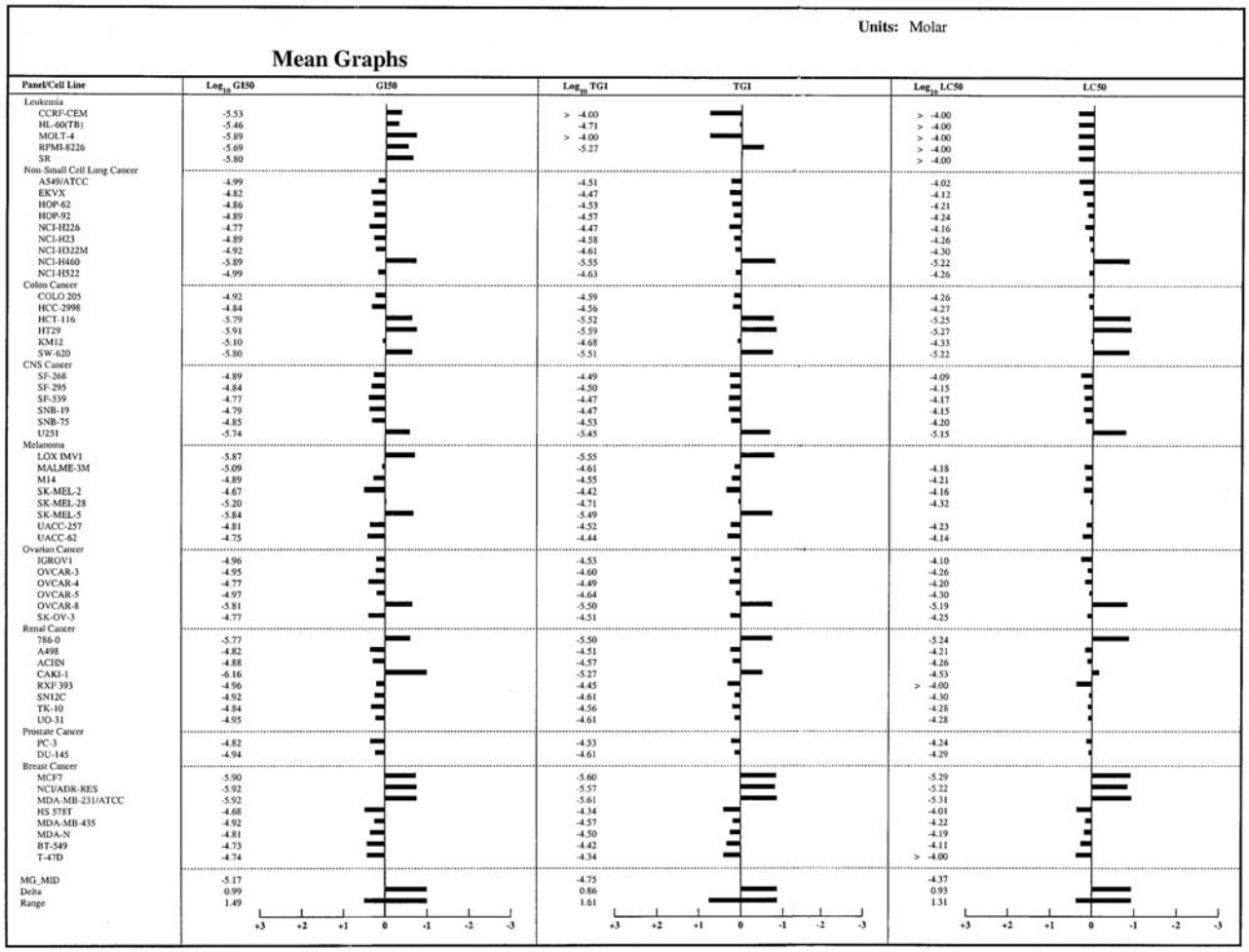

Figure 2. *Mean graph of compound 10a in the NCI in vitro human tumor cell line panel. GI_{50}, TGI and LC_{50} are interpolated log10 values representing concentrations at which the percentage growth is +50, 0 and -50%, respectively. Each bar indicates whether the sensitivity of the cell line is greater (bar to the right) or less (bar to the left) than the average response.*

continuous exposure in 0.2 ml of medium. In each assay, six control plates received the vehicle only; drug-treated groups were plated in triplicate in three concentrations: 0.1, 1 and 10 μg/ml. Drug effects were expressed as percentage survival obtained by comparing the mean number of colonies in treated plates with the mean number of colonies of control plates (T/C%). Cytotoxicity was considered to be significant if the compound reduced colony formation to less than 30% of the control value (T/C <30%).

The composition of the panel was based more on the sensitivity of the lines to standard anticancer agents than on ensuring that frequently occurring human tumor types were represented. The panel consisted of the sensitive non-small cell lung carcinoma LXFL 529, two intermediately sensitive lines, small cell lung carcinoma LXFS 538 and melanoma MEXF 989, and three resistant lines, colorectal adenocarcinoma CXF 1103, ovarian adenocarcinoma OVXF 1023 and renal cancer RXF 423. Most of the standard anticancer agents are active at a dose of ≤ 1 μg/ml.

In vivo antitumor studies. All of the animal experiments were carried out under a project license issued by the Home Office, London, UK or local authorities in Freiburg and Berlin, Germany. According to the local Animal Experimentation Rules, animals were killed before the tumor diameter exceeded 20 mm in any plane.

Tumor xenografts. The human ovarian xenograft, PXN/109TC, grown subcutaneously (*s.c.*) in female Balb/c nude mice, two human breast carcinomas, MT-1 and MCF-7, grown in female Ncr nu/nu mice, and the murine colon adenocarcinoma MAC 15A grown *s.c.* in male NMRI nude mice, were used. PXN/109TC, which was derived from continuous *in vitro* growing cell line CH1 by *s.c.* injection of 5 x 10^6 cells, is sensitive to cisplatin, carboplatin and iproplatin (19). MT-1 is an undifferentiated, medullar mammary carcinoma, estrogen receptor-negative and chemosensitive. MCF-7 is derived from an *in vitro* growing cell line, estrogen receptor-positive and fairly chemo-resistant (20). MAC15A is a rapidly growing, poorly-differentiated chemo-resistant tumor originally developed as an ascitic tumor (21).

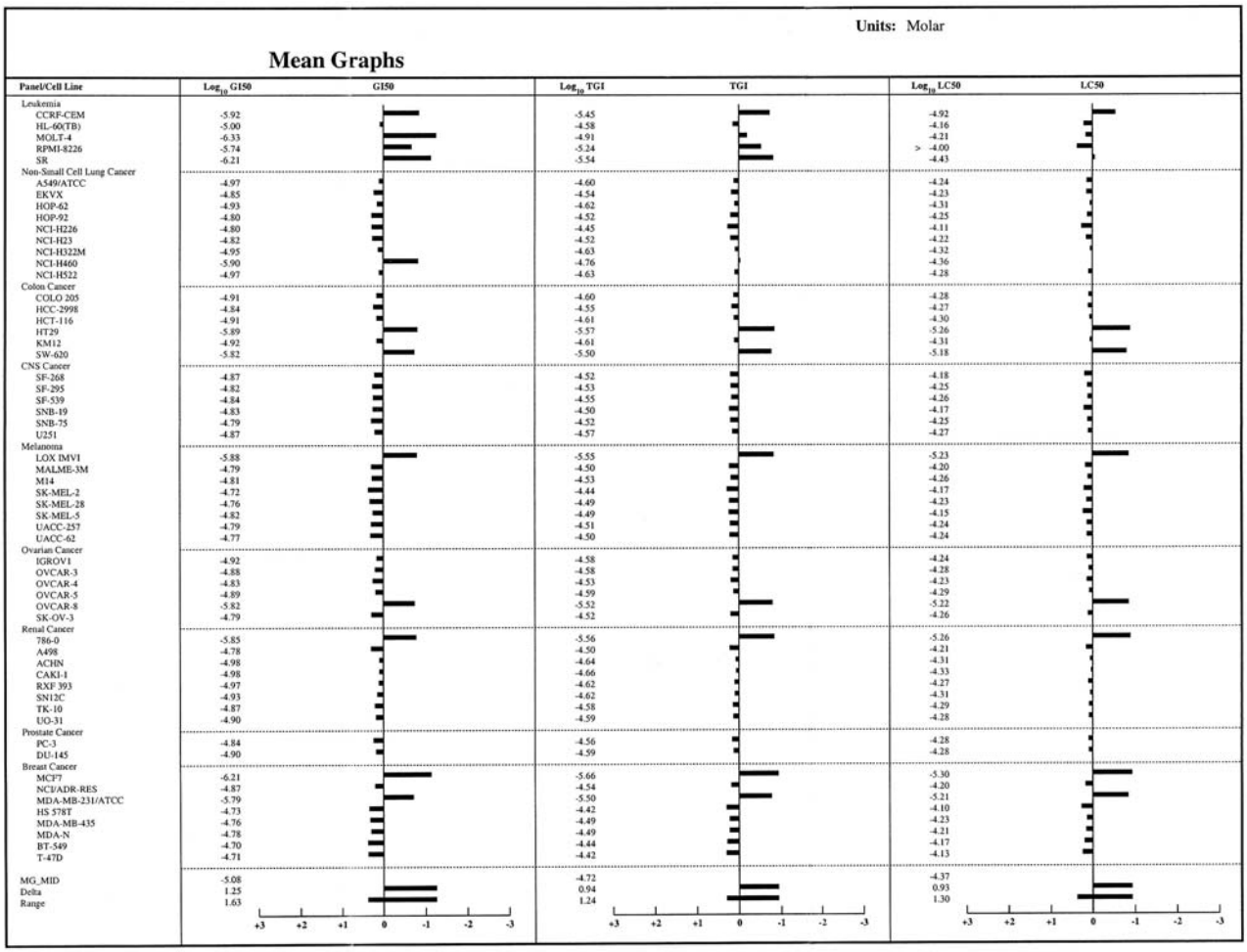

Figure 3. *Mean graph of compound 10c in the NCI in vitro human tumor cell line panel.*

Assessment of antitumor activity

PXN/109T/C. This was performed as described previously (19). Briefly, nude mice bearing 35-100mm^3 subcutaneous PXN/109T/C ovarian carcinoma xenografts were randomized to receive either the compound 10a at doses of 25, 50 and 100 mg/kg (5 mice/group; intraperitoneal (*i.p.*) dosing as a fine suspension in saline) or no drug (controls; 10 mice/group). The compound 10a was administered weekly x4 and tumor volumes determined weekly by caliper measurements. The two longest diameters (a and b) at right angles were measured, volumes calculated from: $V=axb^2 \times \pi/6$ and normalized to the volume at the start of treatment (day 0) to produce relative tumor volumes. Growth delays, the difference in time for control and treated tumors to double in volume and 28-day treated/control (T/C) ratios were determined.

Human mammary carcinomas. Female Ncr nu/nu mice with an average age of 5 weeks were used for the transplantation of the human breast carcinomas MT-1 (estrogen receptor-negative) and MCF-7 (estrogen receptor-positive). MT-1 was transplanted as fragment *s.c.* into the left flank of anesthetized (etomidat) mice. Inoculation of MCF-7 was performed with 10^7 cells/mouse from *in vitro* culture *s.c.* Animals bearing MCF-7 tumors received additionally 0.5 mg/kg estradiol/week intramuscularly as hormone supplementation.

Animals bearing MT-1 tumors were treated with doses of 0, 50 and 100 mg/kg of compound 10a (8 mice/group), dissolved in saline and 10% Tween 80, *i.p.* on days 0 and 7. The dose levels were reduced to 25 and 50 mg/kg 10a (8 mice/group) for the animals bearing MCF-7 tumors due to toxic deaths at higher dose levels. Adriablastin was used as reference compound and given *i.v.* at a dose level of 8 mg/kg on days 0 and 7 (n=6).

When the tumors reached palpable sizes (4-5 mm in diameter), animals were randomly allocated into treatment groups. Tumor growth was followed twice weekly by caliper measurement. The two longest diameters (a and b) were measured and volumes calculated by the formula $a^2 \times b/2$ where a is the smaller and b the larger diameter of the tumor. Volumes of each tumor were normalized to their initial values on day 0 to produce relative tumor volumes. Tumor inhibition was calculated by dividing the relative tumor volumes of treated mice by the control values (optimal T/C ratio).

Table I. *Growth inhibition (GI_{50}) of compounds 10a and 10c (μM) in the NCI panel of human tumor cell lines.*

Tumor type (No. tumor cell lines)	Compound	
	10a	10c
Leukemia (5)	2.1	1.4
Non-small cell lung (9)	10.0	10.0
Colon (6)	4.0	6.1
CNS (6)	10.5	14.6
Melanoma (8)	7.2	12.1
Ovarian (6)	9.2	9.5
Renal (8)	6.9	9.3
Prostate (2)	13.2	13.5
Mammary (8)	6.3	8.5
Mean	6.8	8.3

Table II. *In vitro growth inhibition of compounds 10a, 10c-d against human (DLD-1, CH1 and CH1cis) and murine (Mac 15A and WEHI) tumor cell lines.*

Compound	IC_{50} (μM)				
	DLD-1	CH1[a,b]	CH1cis[a,b,c]	WEHIb)	Mac 15A[b]
10a	0.4	0.62	0.93	0.3	0.5
10c	30	4.5	3.8	nd	nd
10d	0.4	0.69	0.81	0.004	0.18
10e	7	6.4	7.8	nd	nd

[a] after 4-day exposure; [b] reported in (12); [c] resistant to cisplatin; nd, not done

Blood parameters were measured (Coulter counter) three days after each treatment from 4 mice each.

Murine colon adenocarcinoma MAC15A. MAC15A is an ascitic variant of the solid MAC15 but in this study was grown as a solid tumor when ascites cells (1 x 10^6) were injected *s.c.* into NRMI male mice, aged 6-8 weeks. Mice were randomized into treatment groups (7-8 mice/group) when tumors had a mean tumor diameter of 5-7 mm. Tumor volumes were determined twice weekly by caliper measurements of two perpendicular diameters. Volumes were calculated by the formula a^2 x b/2 where a is the smaller and b the larger diameter of the tumor. Volumes of each tumor were normalized to their initial values on day 0 to produce relative tumor volumes. Treated/control ratios were determined. Compound 10a (solubilized in saline or in DMSO/Arachis oil) was given *i.p.* as a single dose of 100 and 150 mg/kg/day on day 0 or at 20 mg/kg/day for 5 subsequent days (days 0-4).

Molecular modeling. Initially compound 10a was constructed with the aid of the Hyperchem 5.01 Plus molecule builder. The initial geometry was computed using a molecular mechanics approximation with the aid of the MM+ force field using the Polak- Ribbiere algorithm. The optimization cycle was repeated until no further change of the final geometry was observed. This geometry was used as starting point for carrying out further computation. In order to elucidate some of the electronic properties of the molecule, semi-empirical calculations were performed. The utilization of MINDO/3, CNDO, AM1 and PM3 Hamiltonias gave significantly different results regarding the four-ring heterocyclic system. In order to verify which result is more accurate, an *ab initio* calculation was carried out using the N-631 basis set. *Ab initio* calculations were performed using the GAMESS v.6 software package (22, 23).

The docking study was performed using all the possible combinations of dinucleotides as a double-strand, namely AA, AT *etc*. The dinucleotides were constructed using the Hyperchem 5.01 Plus nucleic acid builder module and then subjected to geometry optimization using the OPLS force field. The docking was performed by an exhaustive 3-D grid search using the GRAMM 1.03 program.

Results

In vitro antitumor activity. Figures 2 and 3 show the mean graph presentations of GI_{50}, TGI and LC_{50} results of the compounds 10a and 10c in the NCI human tumor cell line panel tested on the same day. The profiles of the compounds are slightly different as well as their mean GI_{50} values: 6.8 μM for 10a and 8.3 mM for 10c. In the mean graph of 10a, clusters of sensitive tumor cell lines corresponding to leukemia, colon and mammary cancer for one or more of the calculated parameters (GI_{50}, TGI, and LC_{50}) were identified. This was less for compound 10c. For instance 5/5 leukemia lines in the GI_{50} mean graph of compound 10a and 4/5 lines in that of compound 10c were more sensitive than the mean values of the compounds, most of them 0.5-1 log. This is for 10a in colon 3/6 and 2/6 for 10c. Three of eight mammary cancer cell lines, MCF7, MCF7/ADR [now called NCI/ADR-RES (24,25)] and MDA-MB-231, were all approximately 1 log more sensitive in the GI_{50}, TGI, LC_{50} mean graphs of 10a compared with the mean value, whereas 2/8 lines were observed for 10c. Table I depicts the average GI_{50} values of 10a and 10c for the various tumor types. The profile and values of the test parameters of 10a (GI_{50}: 4.8 μM) were confirmed in a second independent experiment.

Compound 10e was less potent with GI_{50} values >10 μM and compounds 10b and 10d were not tested in the NCI *in vitro* screen. COMPARE analyses of the GI_{50} profile of 10a and 10c against the standard agent database did not show a significant correlation with agents with a specific mechanism of action. Thus, although the *in vitro* profile of these two compounds in the NCI *in vitro* screen appeared similar, compound 10a had a better overall activity in all the tested cell lines, with the exception of the leukemia where 10c was slightly more potent.

Table III. *In vitro cytotoxicity of compounds 10a, 10c-e in a panel of six human tumor xenografts.*

Dose µg/ml	Xenografts*active/total				
	10a	10c	10d	10e	Mitoxantrone
0.1	0/6	0/6	0/6	0/6	4/6 (LXFL, LXFS, MEXF, OVXF)
1	1/6 (LXFL)	2/6 (CXF, MEXF)	0/6	0/6	4/6 (LXFL, LXFS, MEXF, OVXF)
10	4/6 (LXFL, LXFS, MEXF, OVXF)	3/6 (CXF, LXFS, MEXF)	2/6 (LXFL, MEXF)	1/6 (LXFL)	4/6 (LXFL, LXFS, MEXF, OVXF)

* colorectal cancer CXF 1103, non-small cell lung cancer LXFL 529, small cell lung cancer LXFS 538, melanoma MEXF 989, ovarian cancer OVXF 1023 and renal cancer RXF 423

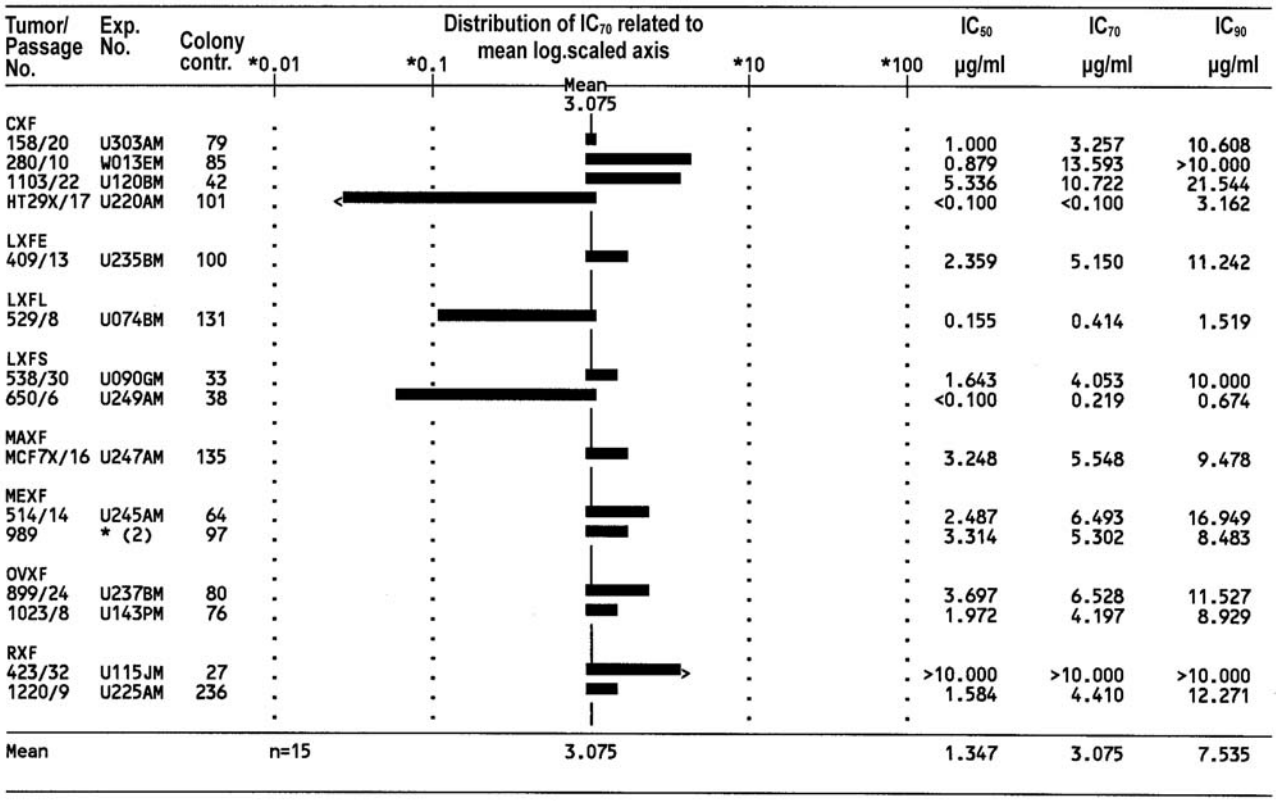

Figure 4. *The IC_{70} profile of compound 10a in the clonogenic assay against a panel of 15 human tumor xenografts. The panel consists of colorectal cancers CXF 158, 280,1103 and HT29X, non-small cell lung cancers LXFL 529 and LXFE 409, small cell lung cancers LXFS 538 and 650, mammary cancer MCF7X, melanomas MEXF 514 and 989, ovarian cancers OVXF 899 and 1023 and renal cancers RXF 423 and 1220. Each bar indicates whether the sensitivity of the cell line is greater (in contrast to the NCI mean graph: bar to the left) or less (bar to the right) than the average response.*

The results of the evaluated imidazothioxanthenones in the NCI screen were partially in agreement with those obtained in a panel of murine and human tumor cell lines also using a monolayer culture system. The profile of the compounds 10a, 10c-e did show differential activity towards the tested tumor cell lines (Table II). Compounds 10a and 10d were the most potent and inhibited tumor cell growth below 1 µM. They were specifically active in the mouse

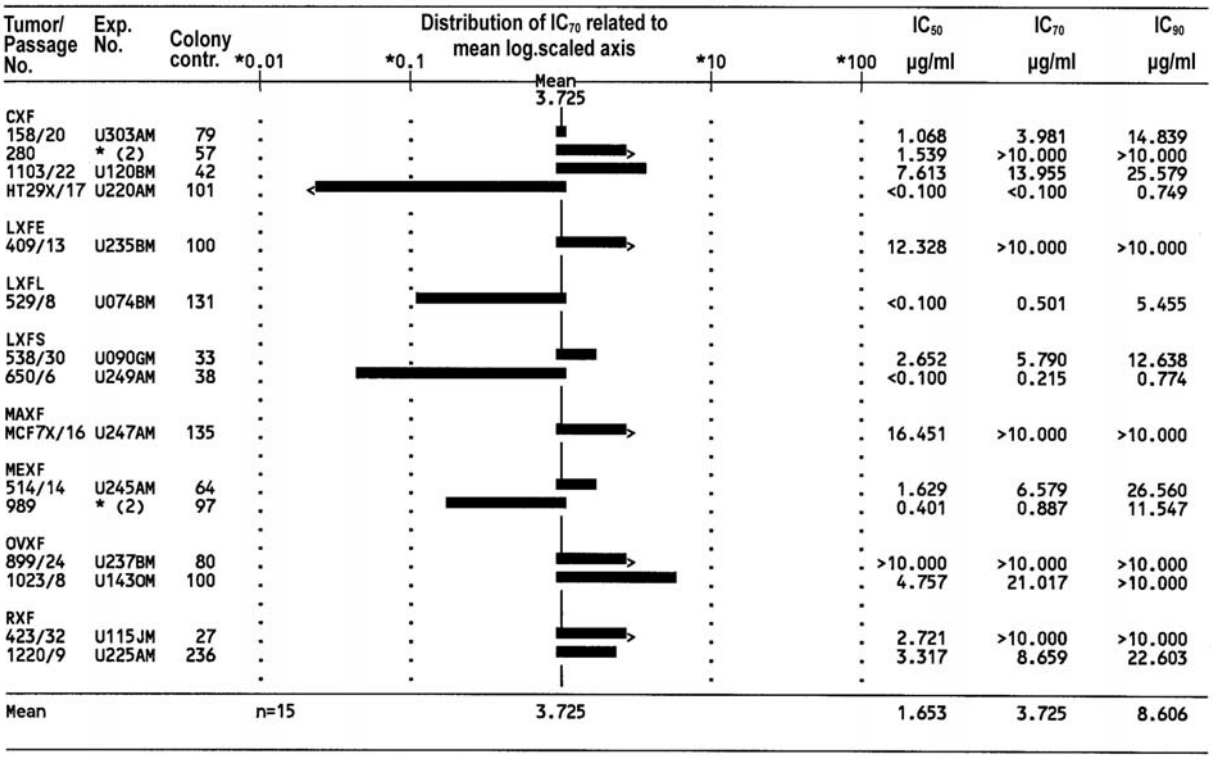

Figure 5. *The IC_{70} profile of compound 10c in the clonogenic assay against a panel of 15 human tumor xenografts.*

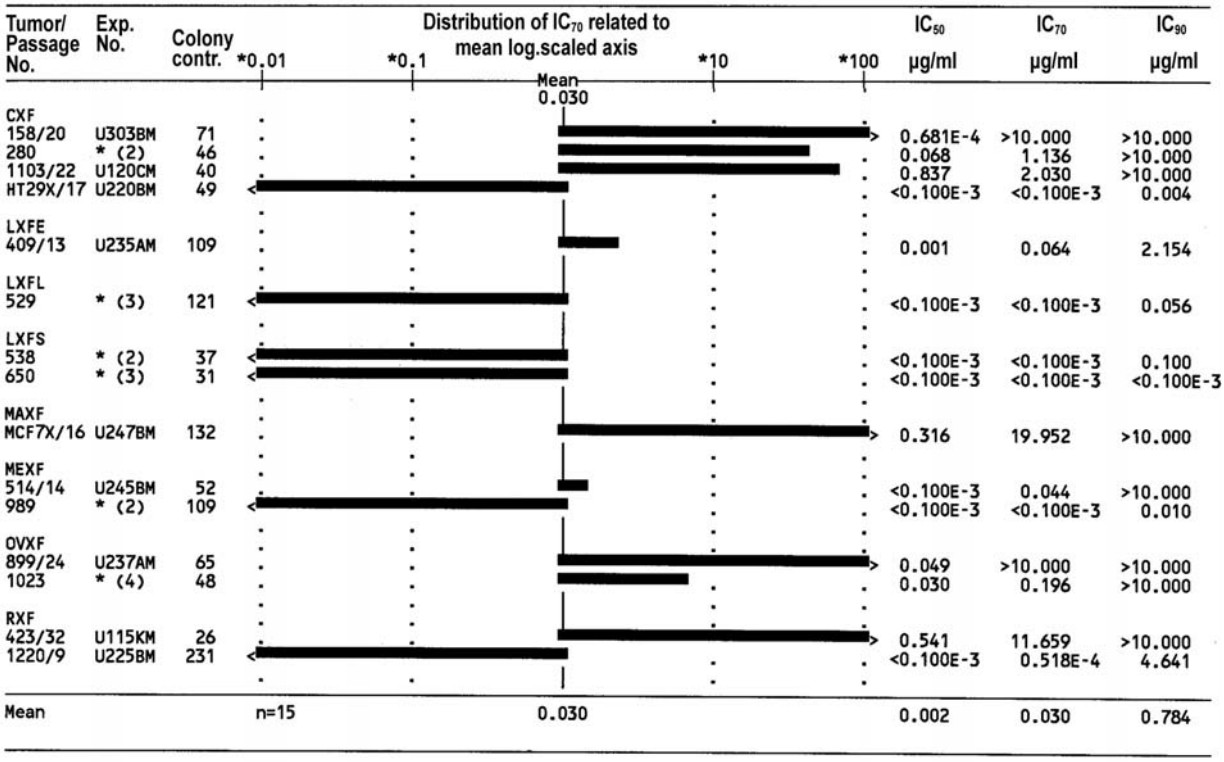

Figure 6. *The IC_{70} profile of reference compound mitoxantrone in the clonogenic assay against a panel of 15 human tumor xenografts.*

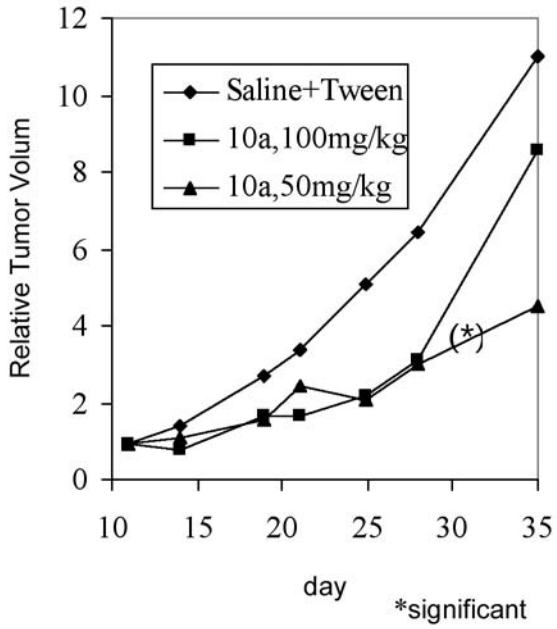

Figure 7. *Antitumor activity of compound 10a against human mammary carcinoma MT-1, i.p. administration on days 0 and 7.*

leukemia WEHI and the human colon carcinoma DLD-1. Analogs 10c and 10e were not very potent, but did exhibit antiproliferative effects. All compounds had a similar IC_{50} value comparing the ovarian cancer parent CH1 line with its cisplatin-resistant subline CH1cis.

Further experiments confirmed the *in vitro* activity of compounds 10a and 10c in a clonogenic assay using human tumor xenografts (Table III). In six different tumor types (colon, non-small and small cell lung, melanoma, ovarian and renal cancer) activity (T/C <30%) was established, starting at a dose level of 0.1 μg/ml. At the dose of 1 μg/ml, activity was observed for 10a in 4/6 and for 10c in 3/6 tumors. The mean IC_{70} value of these compounds was 4.0 and 4.4 μg/ml, respectively. Analogs 10d and 10e were less potent, showing activity only at the dose of 10 μg/ml in 2/6 and 1/6 tumors. The reference compound mitoxantrone was more potent than the imidazothioxanthenones. It was active at all three dose levels (0.1, 1, 10 μg/ml) in 4/6 tumors and the mean IC_{70} value was 0.4 μg/ml (Table III).

In conclusion, compounds 10a and 10c are effective agents in the chemo-sensitive tumor LXFL 529 and intermediate sensitive tumor LXFS 538 and MEXF 989 lines. Additionally, compound 10a showed activity in the chemo-resistant OVXF1023 tumor xenograft.

In a follow-up study, compounds 10a and 10c were further investigated in nine additional human tumor xenografts. The final panel of 15 xenografts comprised 4 colorectal, 2 non-small cell lung, 2 small cell lung, 2 melanoma, 1 mammary, 2 ovarian and 2 renal cancer xenografts. The overall results of the compounds in the panel showed that 10a was active at the dose of 0.1 μg/ml in 1/15 tumors, 3/15 at 1 μg/ml and 12/15 xenografts at 10 mg/ml. This was for compound 10c 1/15, 4/15 and 8/15 tumors at the doses of 0.1, 1 and 10 μg/ml, respectively. Mitoxantrone was active in approximately 50% of the xenografts at concentrations ranging from 0.001 to 10 μg/ml. Figures 4, 5 and 6 display the activity profiles of the three compounds. The mean IC_{70} value was for 10a 3.1 μg/ml, for 10c 3.7 μg/ml and 0.03 μg/ml for mitoxantrone. The most sensitive tumors to both compounds were human colon cancer HT29, small cell lung cancer LXFS 650 and non-small cell lung cancer LXFL 529. These data confirm that the profile of 10a and 10c are similar but that 10a is slightly more potent at higher concentrations compared with 10c.

In summary, compounds 10a and 10c were the most potent ones in the investigated series of imidazothioxanthenones. The cytotoxicity profiles of these compounds in the various screens differ slightly, but both show differential activity for leukemia, colon and mammary cancer.

In vivo activity. After establishing that compound 10a was the most potent *in vitro*, the antitumor activity of the compound was investigated in various tumor models *in vivo*.

Table IV. *Antitumor activity of compound 10a against human mammary cancer MT-1 in vivo.*

Group	Dose mg/kg	Route & schedule	BWC (%) d 0-11	Death (day)	Optimal T/C%	TD (days)	WBC (d 3) (10^6/ml)	Throm (d 3) (10^6/ml)
Control	vehicle*	*i.p.*, d 0,7	+9	0/9	-	6.5	10.1	850
10a	100	*i.p.*, d 0,7	-14	3/8 (1-3)	45	7.2	9.6	640
	50		-8	1/8 (15)	44**	16.0	8.0	778

TD, tumor doubling-time; BWC, body weight change; WBC, white blood cell count; Throm, thrombocyte count; d, day
*, saline + 10% Tween 80; **, $p<0.05$

Table V. *Antitumor activity of compound 10a against human mammary cancer MCF-7 in vivo.*

Group	Dose mg/kg	Route & schedule	BWC (%) d 0-11	Death (day)	Optimal T/C%	TD (days)	WBC (d 3) (10^6/ml)	Throm (d 3) (10^6/ml)
Control	vehicle*	i.p., d 0,7	+3	0/8	-	14.7	5.8	797
10a	50	i.p., d 0,7	-3	0/8	65	20.1	6.1	700
	25		-2	0/8	59	17.4	4.3	845
Adriablastin	8	i.v.,d 0,7	-17	0/6	29**	>23	2.7**	994

TD, tumor doubling-time; BWC, body weight change; WBC, white blood cell count; Throm, thrombocyte count; d, day
*, saline + 10% Tween 80; **, $p<0.05$

Human ovarian cancer PXN/109T/C. Compound 10a was administered *i.p.* weekly x4 at doses of 25, 50 and 100 mg/kg/day. While no animal weight loss and deaths were observed at the 25 and 50 mg/kg doses, following a single dose of 100 mg/kg, mice became very sick and died or were culled 24 h post administration. In addition, at 50 mg/kg, irritation at the time of injection was noted. Thus, 50 mg/kg/day is considered to be the approximate maximum tolerated dose (MTD).

The antitumor activity of 10a was dose-dependent in the ovarian cancer xenograft PXN/109T/C. At the MTD the 28-day T/C value was 52% and the growth delay only 1.7 days on a tumor doubling-time of 5 days for the control. The lower dose of 25 mg/kg/day had a T/C of 69% and 1.7 days growth delay. Thus, compound 10a was only marginally active against the PXN/109TC tumor model at the MTD.

Human mammary cancers MT-1 and MCF-7. Compound 10a was administered *i.p.* weekly x2 at dose levels of 50 and 100 mg/kg/day to mice bearing the estrogen receptor-negative tumor MT-1. The dose of 100 mg/kg/day caused the deaths of 3/8 animals within 4 days after the first injection and a body weight loss of 14%. The lower dose of 50 mg/kg/day induced the death of one animal (day 15), 8% body weight loss and a slight decrease in blood leukocytes and platelets. The T/C value was 44% and the growth delay 9.5 days, whereas the tumor doubling-time of the control was 6.5 days (Table IV, Figure 7). This means that 10a was moderately active in the MT-1 tumor.

In the estrogen receptor-positive MCF-7 mammary cancer, 25 and 50 mg/kg/day of compound 10a did not cause any death nor a significant effect on the numbers of leukocytes and platelets. The body weight loss remained below 3% . Compound 10a had no distinct effect on tumor growth inhibition. The T/C values ranged from 59-65% and the growth delays from 2.7-5.4 days with a control that doubled in volume in 14.7 days (Table V). The reference compound adriablastin caused a significant growth inhibition (T/C 28%, growth delay >23 days) and a significant decrease in leukocyte number.

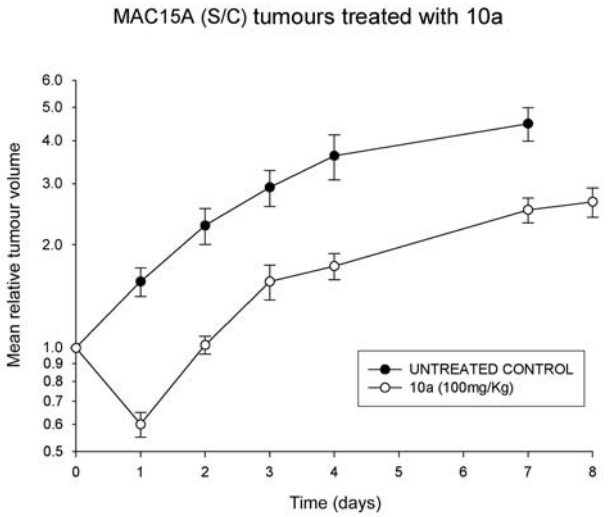

Figure 8. *Antitumor activity of compound 10a against murine colon carcinoma MAC15A, i.p. administration on day 0.*

In conclusion, the test compound 10a showed antitumour activity in one out of two mammary carcinoma xenografts. At the MTD of 50 mg/kg, *i.p.* administration weekly x2, it induced a moderate but significant tumor growth inhibition in MT-1 and no antitumor effect in MCF-7.

Murine colon carcinoma MAC15A. The antitumor effect of compound 10a was also assessed against MAC15A, a rapid growing solid tumor established from ascitic cells implanted subcutaneously in NMRI mice. In a first experiment a single *i.p.* dose of 100 mg/kg/day (solubilized in saline) seemed to be the MTD, because it induced a body weight loss of 10-

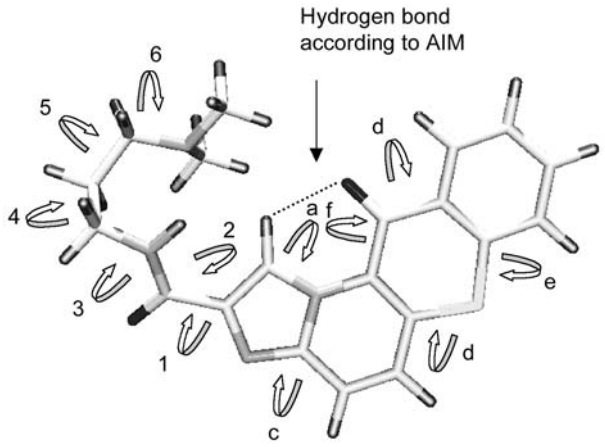

Figure 9. *Optimized structure at the HF/6-31g level geometry of the 10a molecule after a MM+ molecular mechanics conformational search for the determination of the side-chain conformation.*

Table VI. *Selected dihedral angles and bond distances of compound 10a as calculated at the N31-6 ab initio level of theory after an MM+ conformational search.*

Dihedral angle	Bond length (A)	Dihedral angle (°)
1		149.1
2		166.3
3		85.9
4		62.5
5		70.1
6		74.9
a		179.4
b	1.485	175.7
c		197.7
d	1.780	-176.9
e	1.786	177.1
f	1.492	175.9

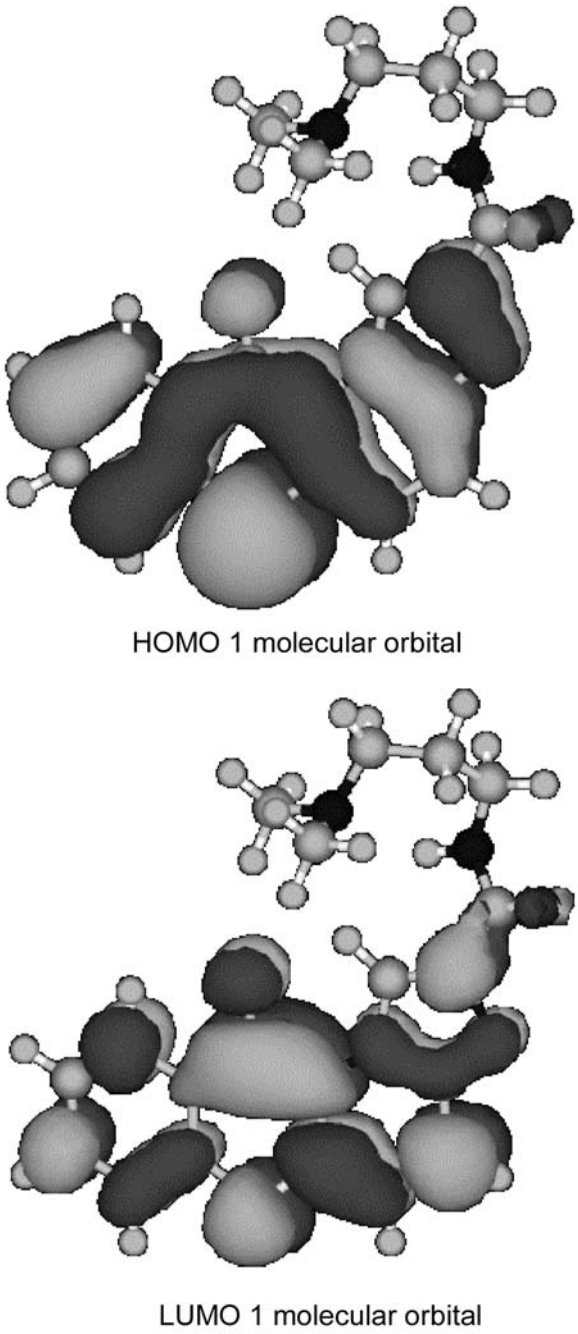

Figure 10. *Spreading of the HOMO and LUMO orbitals indicating the aromaticity of the molecule 10a.*

15% and 1 animal out of 5 died. The MTD resulted in a decrease in tumor volume one day after the *i.p.* administration of 10a, which is rather unusual for this chemo-resistant tumor (T/C 40%). Next, the tumor increased in volume reaching its starting volume at day 2 and 2-3x this volume at days 7 and 8. The volume of the tumor in the treated mice remained well below that of the control mice (Figure 8). In a follow-up experiment with dose levels of 100 and 150 mg/kg/day (10a solubilized in DMSO and Arachis oil), the antitumor activity could not be confirmed, because both dose levels caused the death of 50% or more of the mice. These doses were therefore not evaluable for antitumor activity. Daily *i.p.* treatment x5 with 20 mg/kg/day of 10a caused a body weight loss of 6% and no animals died. However, no antitumor activity was observed, the optimal T/C was 83%.

In conclusion, compound 10a is inactive against the chemo-resistant tumor MAC15A *i.p.* dx5 at 20 mg/kg/d, but active after a single *i.p.* injection of 100 mg/kg/day when 10a was solubilized in saline.

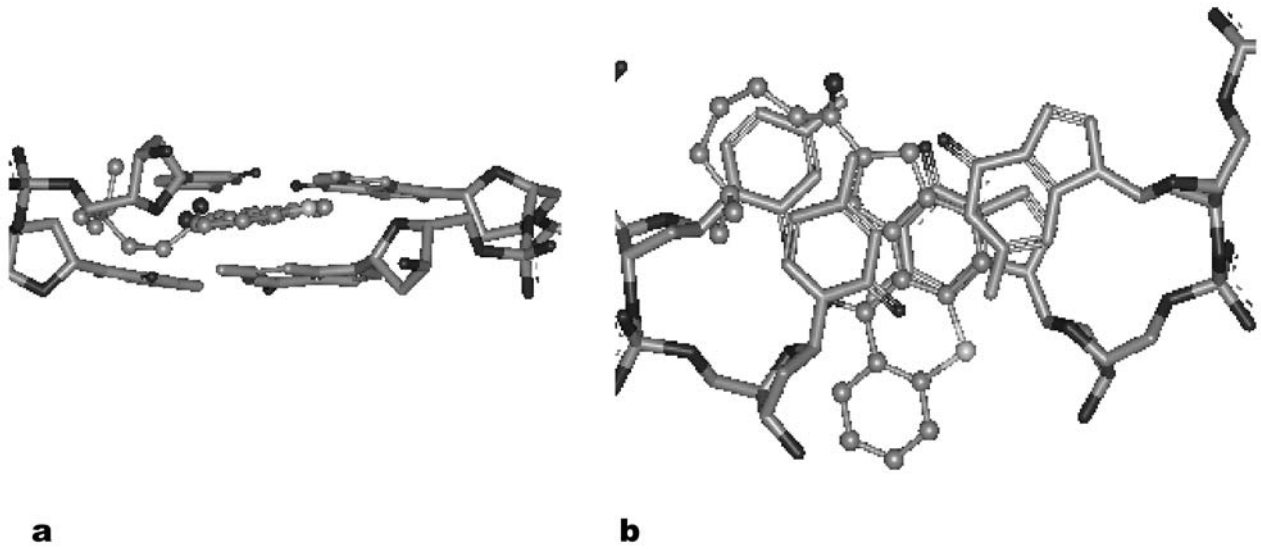

Figure 11. *Structure of the intercalation dinucleotide (AT) - 10a complex a. from the minor groove, b. from a plane perpendicular to the plane of the bases.*

Molecular modeling. In the effort to determine the lowest energy conformation of compound 10a, a random walk conformational search starting from the AM1 optimized geometry was performed. Five torsional angles were considered (shown in Figure 9) which describe adequately the mobility of the side-chain. For computational simplicity, the molecular mechanics MM+ force field as implemented in Hyperchem 5.01 was used. The molecule was allowed to adopt 1000 randomly generated conformations. The lowest conformation was found to be the one shown in Figure 9. There is only a 0.185 kcal/mol energy barrier between the first and the tenth lowest conformation. The corresponding dihedral angles 1, 2, 3, 4 and 5 (denoted in Figure 9) differ at maximum only by 3, 6, 20, 1 and 1 degrees between the ten aforementioned lowest conformations, indicating that the proposed conformational state is the global minimum. Finally, in order to establish accurately the geometry and the electronic properties of the lowest conformation, the lowest energy molecule resulting from the conformational search was optimized at the AM1 and finally at the *ab initio* 6-31G level of theory. The resulting geometry (selected dihedral angles and bond lengths) is found in Table VI.

It is generally accepted that chromophore planarity is an essential requirement for efficient insertion of the molecule between the base pairs of the double helix. It can be easily anticipated from the results presented in Table VI that the 10a molecule adopts an essentially planar conformation for the central heterocyclic system. The respective angles between the thiopyranone and the benzene nuclei lie between 175.7 and 177.1˚ as calculated from the *ab initio* calculation. The aromaticity-planarity of the molecule can also be anticipated by visualizing the spreading of the frontier molecular orbitals HOMO and LUMO. These orbitals are delocalized across the benzene and the imidazole rings (Figure 10) whereas the S atom has a localized HOMO orbital and does not contribute significantly to the aromaticity of the whole system. A second feature is the formation of a hydrogen bond between the thiopyranone carbonyl oxygen and the hydrogen of the imidazole ring. This feature was established using Bader's AIM theory. The existence of this bond essentially creates one more ring, increasing thus the inflexibility of the molecule.

Table VII. *Relative intercalation energies for the three preferential conformations of compound 10a as calculated by the GRAMM 1.03 docking program. (The bold data refer to conformations that give an intercalation complex).*

	1	2	3
TG	-129	-127	-126
CC	-118	-118	-115
AC	-117	-117	-117
GG	-117	-116	-115
AT	-116	-116	-114
GC	-115	-110	-110
TC	-113	-112	-111
AG	-112	-107	-107
TT	-112	-112	-112
AA	-110	-110	-110

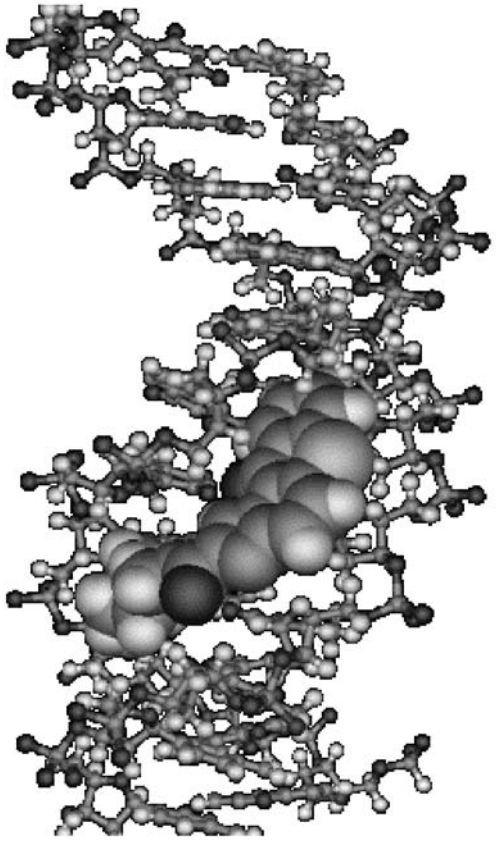

Figure 12. *Structural model of 10a bound to the minor grove of a DNA oligonucleotide. The long axis of the molecule adopts a parallel orientation to the minor groove of DNA strands.*

Another important feature is the conformation of the side-chain. The side-chain adopts a bend conformation instead of a linear one. This feature enables the molecule to be "anchored" with the amino group to the negatively-charged backbone of the DNA molecule and stabilizes the supramolecular system.

The lowest energy conformation determined from the *ab initio* optimization was used as input for the docking study. The docking study indicates that 10a could act as an intercalating agent to the DNA molecule (Figure 11a and 11b). The relative free energies of the binding to dinucleotides are presented in Table VII. Nevertheless docking to the nucleotide sequence GGAATTGCCTCA suggested that the molecule could also act as a minor groove binder (Figure 12). Presumably the flanking nucleotide bases provide the driving force for intercalation. It can be also assumed that binding to the minor groove of the DNA strand initiates some local conformational changes that can facilitate the intercalation procedure (Figure 11a)

Discussion

This study has demonstrated that the aforementioned imidazothioxanthones have potent cytotoxic activity against a panel of cell lines. Moreover, analogues bearing highly protonable ends *i.e.* 10a and 10c, followed by 10d, proved to be more potent than the morpholin analog 10e. Highly basic and not bulky substituents at the side-chain *i.e.* dimethylaminogroup enhances activity, since compound 10a demonstrated a better overall *in vitro* effect. The substantial *in vitro* activity of compound 10a along with its high DNA-binding affinity (12), led to the inclusion of this compound in *in vivo* tests. We investigated antitumor activity against ovarian cancer PXN/109T/C, mammary cancers MT-1 and MCF-7 and murine colon adenocarcinoma MAC 15A.

A single dose of 100 mg/kg/day, given *i.p.*, was the MTD in murine tumor MAC15A-bearing mice, whereas it was 50 mg/kg/day in the three human tumor models, administered weekly x2 or x4.

At the MTD compound 10a was only marginally active against human ovarian cancer PXN/109T/C, whereas a moderate but significant tumor growth inhibition in the estrogen receptor-negative human mammary carcinoma MT-1 was observed. The test compound was rather inactive in the estrogen receptor-positive human mammary carcinoma MCF-7. The rather chemo-resistant murine tumor MAC 15A was sensitive to compound 10a, since one single dose of 100 mg/kg resulted in a significant decrease in tumor volume one day after the *i.p.* administration.

The fact that compound 10a, when administered *i.p.*, showed *in vivo* antitumor activity in two-three of the four tested tumor models suggests that further experiments including more estrogen receptor-negative breast tumors, colon carcinomas and cross-resistance profiles are warranted.

The computational chemistry study implies that compound 10a possesses an intercalator structure similar to that of other anticancer drugs such as mitoxanthrone. The molecule includes a planar aromatic system in its structure, which can be inserted between the base pairs of DNA and a flexible side-chain with an amine group, that could be positively-charged and bind to the negatively-charged DNA backbone. The results were confirmed by both semi-empirical and *ab initio* methods in order to gain greater accuracy. The docking study involving all the possible dinucleotides confirmed that 10a could act as an intercalator or as a minor groove binder when a decanucleotide in the docking study. The results indicate that the 10a molecule can bind to DNA and therefore can support the pharmacological data presented. Further experiments, like dichroism and fluorescence energy transfer methods, can potentially distinguish intercalative from groove binding.

Acknowledgements

The Developmental Therapeutic Program, DCT, NCI, Bethesda, MD, U.S.A. is gratefully acknowledged for the *in vitro* screening data. The other *in vitro* and *in vivo* experiments were performed under the auspices of the Screening and Pharmacology Group of the EORTC.

References

1 Zee-Cheng RK and Cheng CC: Antineoplastic agents. Structure-activity relationship study of bis(substituted aminoalkylamino) anthraquinones. J Med Chem *21*: 291-294, 1978.
2 Showalter HD, Johnson JL, Werbel LM, Leopold WR, Jackson RC and Elslager EF: 5-[(Aminoalkyl)amino]-substituted anthra[1,9-cd]pyrazol-6(2H)-ones as novel anticancer agents. Synthesis and biological evaluation. J Med Chem *27*: 253-255, 1984.
3 Leopold WR, Nelson JM, Plowman J and Jackson RC: Anthrapyrazoles, a new class of intercalating agents with high-level, broad spectrum activity against murine tumors. Cancer Res *45*: 5532-5539, 1985.
4 Archer S, Miller KJ, Rej R, Periana C and Fricker L: Ring-hydroxylated analogues of lucanthone as antitumor agents. J Med Chem *25*: 220-227, 1982.
5 Chen Q, Deady LW, Baguley BC and Denny WA: Electron-deficient DNA-intercalating agents as antitumor drugs: aza analogues of the experimental clinical agent N-[2-(dimethylamino) ethyl]acridine-4-carboxamide. J Med Chem *37*: 593-597, 1994.
6 Atwell GJ, Rewcastle GW, Baguley BC and Denny WA: Potential antitumor agents. *In vivo* solid-tumor activity of derivatives of N-[2-(dimethylamino)ethyl]acridine-4-carboxamide. J Med Chem *30*: 664-669, 1987.
7 Antonini I, Polucci P, Kelland LR, Spinelli S, Pescalli N and Martelli S: N4-(omega-Aminoalkyl)-1-[(omega-aminoalkyl) amino]-4-acridinecarboxamides: novel, potent, cytotoxic, and DNA-binding agents. J Med Chem *43*: 4801-4805, 2000.
8 Lee HH, Palmer BD, Boyd M, Baguley BC and Denny WA: Potential antitumor agents. Synthesis and antitumor evaluation of dibenzo[1,4]dioxin-1-carboxamides: a new class of weakly binding DNA-intercalating agents. J Med Chem *35*: 258-266, 1992.
9 Spicer JA and Denny WA: Synthesis of tetracyclic benzodioxins as potential antitumour agents. Anticancer Drug Des *15*: 453-458, 2000.
10 Rewcastle GW, Denny WA and Baguley BC: Potential antitumor agents. Synthesis and antitumor activity of substituted phenazine-1-carboxamides. J Med Chem *30*: 843-851, 1987.
11 Gamage SA, Spicer JA, Rewcastle GW, Milton J, Sohal S, Dangerfield W, Mistry P, Vicker N, Charlton PA and Denny WA: Structure-activity relationships for pyrido-, imidazo-, pyrazolo-, pyrazino-, and pyrrolophenazinecarboxamides as topoisomerase-targeted anticancer agents. J Med Chem *45*: 740-743, 2002.
12 Varvaresou A, Tsotinis A, Siatra-Papastaikoudi T, Papadaki-Valiraki A, Thurston DE, Jenkins TC and Kelland LR: Novel imidazothioxanthones: synthesis, DNA binding and cytotoxicity. Bioorg Med Chem Lett *6*: 865-870, 1996.
13 Monks A, Scudiero D, Skehan P, Shoemaker R, Paull K, Vistica D, Hose C, Langley J, Cronise P, Vaigro-Wolff A, Gray-Goodrich M, Campbell H, Mayo J and Boyd M: Feasibility of a high-flux anticancer drug screen using a diverse panel of cultured human tumor cell lines. J Natl Cancer Inst *83*: 757-766, 1991.
14 Boyd MR and Paull KD: Some practical considerations and applications of the National Cancer Institute *in vitro* anticancer drug discovery screen. Drug Dev Res *34*: 91-109, 1995.
15 Alley MC, Scudiero DA, Monks A, Hursey ML, Czerwinski MJ, Fine DL, Abbott BJ, Mayo JG, Shoemaker RH and Boyd MR: Feasibility of drug screening with panels of human tumor cell lines using a microculture tetrazolium assay. Cancer Res *48*: 589-601, 1988.
16 Mosmann T: Rapid colorimetric assay for cellular growth and survival: application to proliferation and cytotoxicity assays. J Immunol Methods *65*: 55-63, 1983.
17 Hamburger AW and Salmon SE: Primary bioassay of human tumor stem cells. Science *197*: 461-463, 1977.
18 Berger DP, Henss H, Winterhalter BR and Fiebig HH: The clonogenic assay with human tumor xenografts: evaluation, predictive value and application for drug screening. Ann Oncol *1*: 333-341, 1990.
19 Harrap KR, Jones M, Siracky J, Pollard LA and Kelland LR: The establishment, characterization and calibration of human ovarian carcinoma xenografts for the evaluation of novel platinum anticancer drugs. Ann Oncol *1*: 65-76, 1990.
20 Fichtner I, Naundorf H, Saul GJ, Zschiesche W and Zeisig R: Establishment and characterization of human xenotransplanted breast carcinoma lines: Use for the screening of alkylphosphocholines (APC). Contrib Oncol *51* : 129-133, 1996.
21 Double JA and Cifuentes de Castro L: Chemotherapy of transplantable adenocarcinomas of the colon in mice. II. Development and characterization of an ascitic line. Cancer Treat Rep *62*: 85-90, 1978.
22 Granovsky AA: www http://classic.chem.msu.su/gran/gamess/index.html
23 Schmidt MW, Baldridge KK, Boatz JA, Elbert ST, Gordon MS, Jensen JJ, Koseki S, Matsunaga N, Nguyen KA, Su S, Windus TL, Dupuis M and Montgomery JA: General atomic and molecular electronic structure system. J Comput Chem *14*: 1347-1363, 1993.
24 Scudiero DA, Monks A and Sausville EA: Cell line designation change: multidrug-resistant cell line in the NCI anticancer screen. J Natl Cancer Inst *90*: 862, 1998.
25 Pirnia F, Breuleux M, Schneider E, Hochmeister M, Bates SE, Marti A, Hotz MA, Betticher DC and Borner MM: Uncertain identity of doxorubicin-resistant MCF-7 cell lines expressing p53. J Natl Cancer Inst *92*: 1535-1536, 2000.

Received July 3, 2003
Revised November 19, 2003
Accepted January 16, 2004